Chemical Signatures of the Evolutionary State of Cores

Yuri Aikawa

Department of Earth and Planetary Sciences, Kobe University, Kobe 657-8501, Japan

Abstract.
Recent observations with high angular resolution revealed chemical differentiation in several prestellar cores; while N_2H^+ emission peaks at the core center, CO, CS and CCS emission peaks are offset from the center. Molecular abundances also vary among cores; some cores have high CCS abundance and low N_2H^+ abundance, but others have less CCS and more N_2H^+. Numerical calculations of a chemical-reaction network in contracting cores show that these differentiations and variations can be diagnostics of physical evolution of cores, because molecular abundances and distributions are determined by the balance between the dynamical and chemical time scales. In prestellar cores, low temperatures and high densities cause adsorption of molecules onto grains. Depletion time scale varies among species; early-phase species deplete first because of destruction via gas-phase reactions in addition to the adsorption. N_2H^+ is the last to deplete because of the low adsorption energy of its parent molecule N_2 and depletion of main reactants such as CO. Molecular D/H ratio is another probe of core evolution, since it increases as the adsorption proceeds.

1.   Chemical Differentiation

Density structure in starless cores is estimated from observation of sub-millimeter continuum (Ward-Thompson et al. 1994; Ward-Thompson et al. in this volume) and extinction measurements of background stars (e.g. Alves, Lada, & Lada 2001). It is almost flat in the central region and is proportional to $R^{-(2.0-2.5)}$ in the outer radius. Comparison of these data with molecular line observations has revealed chemical differentiation in several cores. Figure 1 (a) shows one of the most famous examples, L1544. While the dust continuum peaks at the core center, CO and CCS intensities are lower in the center than in the surrounding regions. Distribution of N_2H^+, on the other hand, is similar to that of dust continuum. Observation of rare isotopes and analysis via radiation transfer code indicate that these intensity distributions are not caused by the optical-depth effect, but reflect spatial variation of molecular abundances. Figure 1 (b) shows radial distribution of molecular abundance which is estimated by Tafalla et al. (2002) from their observational data via radiation transfer code. Carbon monoxide and CS are heavily depleted at the core center, while N_2H^+ and NH_3 abundances are constant or even enhanced at the center. Similar differentia-
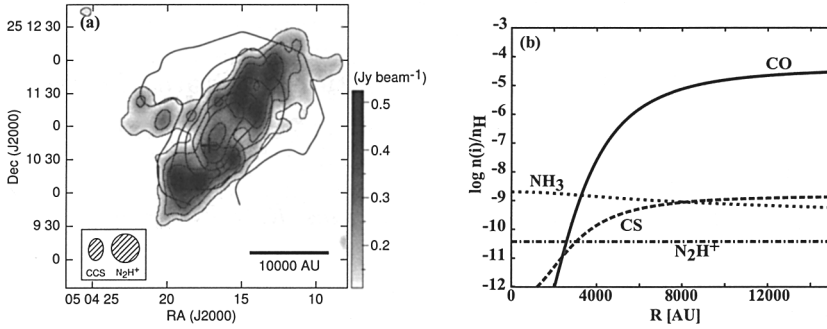
67

Figure 1.   (a) Intensity map of L1544 from Aikawa et al. (2001). The cross indicates a peak position of the dust continuum. The line contour and the gray scale show integrated intensities of N_2H^+ and CCS, respectively. (b) Radial distribution of molecular abundance relative to hydrogen nuclei in L1544.

tion is observed in several prestellar cores such as L1498 (Willacy, Langer & Velusamy 1998) and B68, in which even N_2H^+ is slightly depleted at the core center (Bergin et al. 2002).

Such chemical differentiation is predicted by theoretical modeling of chemical reaction network by Bergin & Langer (1997), and is investigated in contracting core models by Aikawa et al. (2001; 2003), Li et al.(2002) and Shematovich et al. (2003). For example, Figure 2 (a) shows temporal variation of molecular abundances in a fluid parcel which migrates to the central region of a core. The model includes gas-phase reactions, adsorption of gaseous species onto grains, thermal and non-thermal desorption, and grain-surface reaction with modified rates. The adsorption energy of CO is set to be 1780 K (see Aikawa et al. 2003 for model details). Because of the low temperature ($\sim$ 10 K) in the core and temporally increasing density, most gas-phase species, except for hydrogen and helium, are adsorbed onto grains. However, the depletion time scale varies with species. Early-phase species such as CCS, CS, and hydrocarbons deplete first via both the gas-phase reactions (to form CO) and the adsorption. Carbon monoxide is adsorbed onto grains and a fraction of the adsorbed CO is transformed to organic species by grain-surface reactions. Nitrogen species are the last to deplete, because their mother molecule, N_2, has a relatively low adsorption energy on the grain surface. Calculations of molecular evolution in various fluid parcels give radial distribution of abundances (Figure 2 (b)). Carbon monoxide and CS are depleted heavily at the core center, while depletion is not significant for NH_3 and N_2H^+. The model result is in reasonable agreement with the molecular distribution in L1544, which is shown in Figure 1 (b).

2.   Chemical Differentiation as a Probe of Formation and Contraction of Cores

Since prestellar cores are cold, depletion onto grains proceeds with time. Radial distribution of molecules is determined by the balance among dynamical,
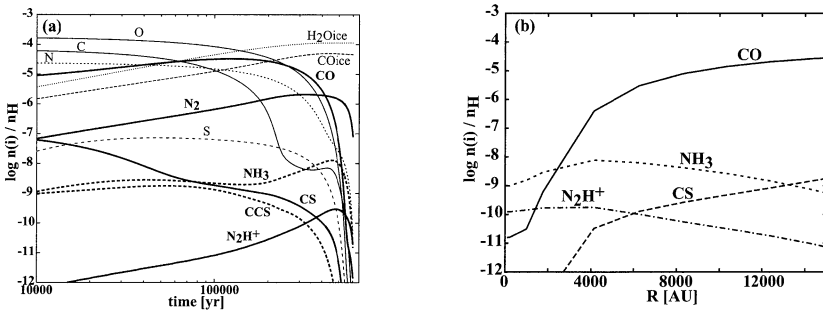
Figure 2.   (a) Molecular evolution in a fluid parcel which migrates from $R = 1.1 \times 10^4$ AU to 100 AU as the core contracts. The contraction is slower than the Larson-Penston flow (Larson 1969; Penston 1969) by a factor of 3. The gas density in the fluid parcel increases from 2×10^4 cm^{-3} to 2.9×10^7 cm^{-3} during the migration. (b) Molecular distribution in the contracting core, when the central density $n_H (= n(H) + 2n(H_2))$ is 3×10^6 cm^{-3}, which is similar to the value in L1544.
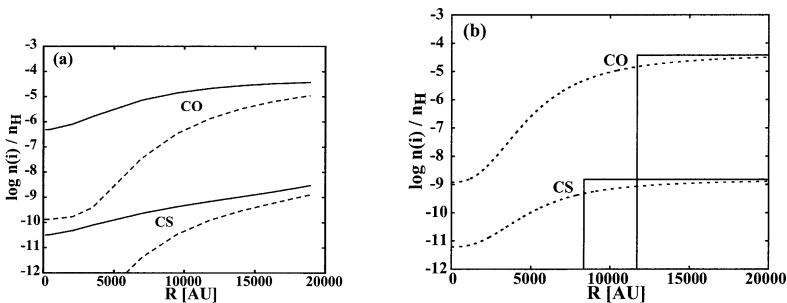

Figure 3.   (a) Molecular distribution in contracting cores, when the central density $n_H (= n(H) + 2n(H_2))$ is 3×10^5 cm^{-3}, which is similar to the value in L1517B. Contraction is slower than the Larson-Penston flow by a factor of 3 (solid lines) and 10 (dashed lines). (b) Molecular distribution in L1517B obtained by Tafalla et al. (2002) (dotted lines) and Tafalla et al. (2003) (solid lines).
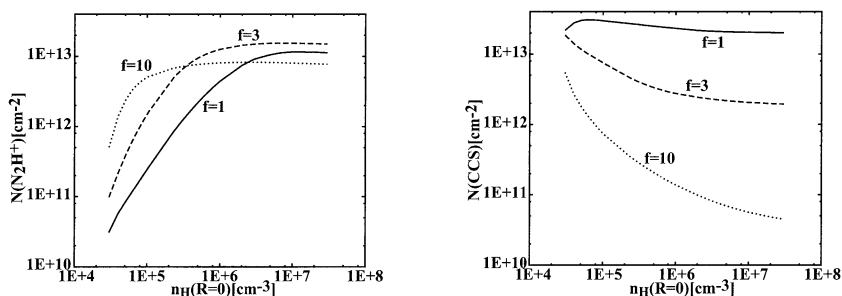
Figure 4.   Column densities of N_2H^+ and CCS as functions of the central density of contracting cores. Contraction is slower than the Larson-Penston flow by a factor f. The column densities are averaged over the radius of 3780 AU and 4340 AU for N_2H^+ and CCS, respectively, referring to the beam sizes of the observations by Caselli et al. (2002) and Suzuki et al. (1992).

chemical and adsorption time scales in cores. Therefore it can be a probe of core formation and evolution. Figure 3 (a) shows molecular distribution in cores with the same central density ($n_H = 3 \times 10^5$ cm^{-3}) but with different contraction time scales. The core with slower contraction suffers heavier depletion at the center and has a larger depleted area. Tafalla et al. (2002; 2003) derived distribution of molecular abundance in L1517B, a starless core with the central density of $\sim 10^5$ cm^{-3} (Figure 3 b). Carbon monoxide and CS decrease inwards rather abruptly. Especially their observation with high spatial resolution (Tafalla et al. 2003) is better reproduced by a step-function distribution (solid lines in Figure 3 b)rather than the exponential decrease of the molecular abundances with gas densities (dotted lines in Figure 3 b), although the molecular emission from the outer radii makes the depth of the abundance drop rather uncertain (the abundance in the inner core is lower than the outer core by a factor of > 20 for $C^{18}O$, Tafalla private communication). The step-function distribution is hard to reproduce with the usual contraction models (i.e. analogues of the Larson-Penston flow or contraction via ambipolar diffusion). The heavy depletion at the center suggests it is a old core with long dynamical time scale, while outer regions with high molecular abundance should be relatively young. It may suggest inhomogeneous core formation with the outer component recently accreted from the ambient cloud. Observation of such depletion pattern with high spatial resolution and high sensitivity is important in order to understand the formation and evolution of cores.

3.   Chemical Variation among Cores

Chemical variation among individual cores is known long before the observations of internal differentiation described above. Comparison with the gas-phase pseudo-time-dependent model suggests that these chemical variations reflect "age" (the time elapsed after the gas becomes relatively dense and is shielded from the interstellar UV), density, and gas-phase C/O ratio (e.g. Suzuki et al.

1992, Hirahara et al. 1992, Pratap et al 1997, Terzieva & Herbst 1998). Here we re-investigate the issue with the recent contracting core model, in which density distribution varies with time and gas-phase C/O ratio is calculated by the gas-dust chemical network.

From the theoretical model of contracting cores, molecular column densities are calculated at each evolutionary stage. Figure 4 (a) shows N_2H^+ and CCS column densities as functions of the central density of the cores with various contraction time scale. As contraction proceeds N_2H^+ increases. It could be a good indicator of core evolution, because its dependence on the contraction model is relatively small. The higher absolute abundance of N_2H^+ in the inner radius (e.g. Figure 2 b) ensures that its column density does not sensitively depend on core size, either. Ammonia column density also tends to increase with evolution in some models, although it is not shown in the figure. On the other hand, CCS column density decreases with contraction and sensitively depends on contraction models.

Table 1.   Observed Molecular Column Densities in Assorted Prestellar Cores

Object	N_2H^+ 10^{12} cm^{-2}	NH_3 10^{14} cm^{-2}	CCS 10^{12} cm^{-2}
L1521E	$< 0.14^a$	0.73^a	28^a
L1521B	1 ± 0.85^b	0.6^c	36^c
L1517B	3 ± 0.3^d, 3.1^e	7^c, 2.1^e	8.6^c
L1400K	4 ± 2^d, 2.7^e	1.8^c, 7.2^e	3.6^c
L1498	8 ± 4^d, 3.0^e	2.3^e	
L1495	6.0^e	2.4^e	
L1544	9 ± 2^d, 7.3^e	1.8^e	20^f
L63	8 ± 4^d	7.9^c	$< 1.7^c$
TMC-2A	11 ± 3^d	10.7^c	3.2^c

[a]Hirota et al. (2002), [b]Takakuwa et al. in prep, [c]Suzuki et al. (1992), [d]Caselli et al. (2002), [e]Tafalla et al. (2002), [f]Ohashi et al. (1999)

Table 1 lists molecular column densities in prestellar cores in the order of increasing N_2H^+ column density. Indeed, NH_3 increases and CCS decreases downwards, as suggested from the theoretical model. Low N_2H^+ column density and high CCS column density in L1521B and E suggest that they are very young cores. Integrated intensity maps show that CCS is centrally peaked in these cores, while it is depleted at the center in other cores such as L1544 (Ohashi 2000; Hirota et al. 2002). Since CCS distribution is centrally peaked only in the early evolutionary stage of the model cores, it strengthen the idea that L1521B and E are young cores and that N_2H^+ can be a good indicator of core evolution.

4.   Deuterium Fractionation

In low-temperature cores molecular D/H ratio increases because some exchange reactions such as $H_3^+ + HD \rightarrow H_2D^+ + H_2$ are exothermic by a few hundred K. CO depletion further enhances the D/H ratio because CO is the main reactant
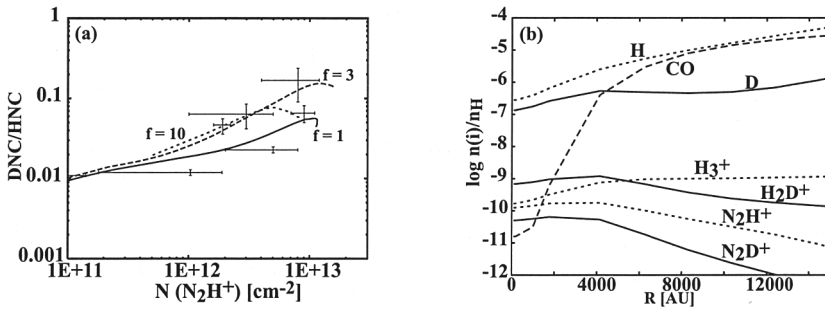
Figure 5.   (a) Column density ratio of DNC to HNC as a function of N_2H^+ column density in contracting cores, while the central density of the cores increases from 3×10^4 cm^{-3} to 3×10^7 cm^{-3}. Contraction is slower than the Larson-Penston flow by a factor f. The column densities are averaged over the radius of 3780 AU and 1400 AU for N_2H^+ and HNC (DNC), respectively, referring to the beam sizes of the observations. The dots with error bars depict observational data of prestellar cores obtained by Caselli et al. (2002) and Hirota et al. (1998; 2003). (b) Molecular distribution in a contracting core when the central density n_H is 3×10^6 cm^{-3}, which is similar to the value in L1544. The contraction is assumed to be slower than the Larson-Penston flow by a factor of 3.

of H_2D^+. Hence in the central region of evolved cores molecular D/H ratio is expected to be much higher than the elemental D/H ratio of 1.5×10^{-5}, and it can be a probe of core evolution. Three observational evidences for the D/H enhancement are reviewed in the following.

Molecular D/H ratio in prestellar cores shows positive correlation with the N_2H^+ column density, which is considered to be a good probe of core evolution from the previous section. Lines in Figure 5 (a) shows N_2H^+ column density and column density ratio of DNC/HNC at the center of contracting core models. Both N_2H^+ and DNC/HNC ratio increase with time. The dots with error bars are observational data of prestellar cores by Caselli et al. (2002) and Hirota at al. (1998; 2003), which are in reasonable agreement with the model predictions.

Caselli et al. (2003) recently detected H_2D^+ at the center of L1544. Its relative abundance to hydrogen is estimated to be as high as 10^{-9}, so that it could be the dominant ion at the core center. Figure 5 (b) shows radial distribution of molecular abundance in a model core. The solid and dashed lines show deuterated and normal species, respectively. Indeed, H_2D^+ is the most dominant ion and has a relative abundance of 10^{-9} at the core center.

In addition to the mono-deuterated species such as DNC and H_2D^+, multiply deuterated species are intensively observed in recent years. Roueff et al. (2000) detected ND_2H in a cold dense core L134N and found the abundance ratio ND_2H/NH_3 of 0.005, which is significantly higher than the value expected from the elemental D/H ratio. Bacmann et al. (2003) detected D_2CO in most prestellar cores of their sample with the abundance ratio $D_2CO/H_2CO \sim 0.01 - 0.1$. Bacmann et al. (2003) also found that the cores with heavier CO depletion have
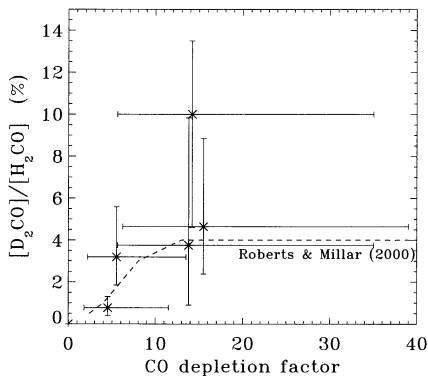
Figure 6.   The abundance ratio of D_2CO/H_2CO and CO depletion factor in prestellar cores. The dashed line is a model prediction by Roberts & Millar (2000). The Figure is from Bacmann et al. (2003).

higher D_2CO/H_2CO ratio (Figure 6), which supports the theoretical prediction that CO depletion enhances the molecular D/H ratio. Mono- and multiply-deuterated species are also abundant in protostellar cores. In IRAS 16293-2422, for example, D_2CO/H_2CO is ~ 0.1 (Ceccarelli. et al. 1998; Loinard et al. 2000) and CHD_2OH/CH_3OH is 0.2$\pm$ 0.1 (Parise et al. 2002). Triply deuterated ammonia is detected in Barnard 1 could and class 0 protostar NGC 1333 IRAS4A with the abundance ratio ND_3/NH_3 of 10^{-3} (Lis et al. 2002; van der Tak et al. 2002). These deuterated species in protostellar cores are desorbed from icy mantle of dust grains, which is formed in prestellar stage via adsorption of gas-phase species and grain-surface reactions. Gas-phase recombination of deuterated ion such as H_2D^+ enhances the abundance ratio of D atom to H atom, which, after their adsorption onto grains, enhances the D/H ratio in hydrogenated species on grain surfaces. Quantitative modeling of the multiply deuterated chemistry is under intensive research (e.g. Roberts, Millar & Herbst 2003).

References

Aikawa, Y., Ohashi, N., Inutsuka, S., Herbst, E., & Takakuwa, S. 2001, ApJ, 552, 639

Aikawa, Y., Ohashi, N., & Herbst, E. 2003, ApJ, 593, 906

Alves, J. F., Lada, C. J., & Lada, E. A. 2001, Nature 409, 159

Bergin, E. A., & Langer, W. D. 1997, ApJ, 486, 316

Bergin, E. A., Alves, J., Huard, T., & Lada, C. J. 2002, ApJ, 570, L101

Bacmann, A., Lefloch, B., Ceccarelli, C., Steinacker, J., Castets, A., & Loinard, L. 2003, ApJ, 585, L55

Caselli, P., Benson, P. J., Myers, P. C. & Tafalla, M. 2002, ApJ, 572, 238

Caselli, P., van der Tak, F. F. S., Ceccarelli, C. & Bacmann, A. 2003, A&A, 403, L37

Ceccarelli, C., Castets, A., Loinard, L., Caux, E., & Tielens, A. G. G. M. 1998, A&A 338, L43

Hirahara, Y., Suzuki, H., Yamamoto, S., Kawaguchi, K., Kaifu, N., Ohishi, M., Takano, S., Ishikawa, S., Masuda, A. 1992. ApJ, 394, 539

Hirota, T., Yamamoto, S., Mikami, H., & Ohishi, M. 1998, ApJ, 503, 717

Hirota, T., Ikeda, M., & Yamamoto, S. 2003, ApJ, in press

Hirota, T., Ito, T., & Yamamoto, S. 2002, ApJ, 565, 359

Larson, R. B. 1969, MNRAS, 145, 271

Li, Z.-Y., Shematovich, V. I., Wiebe, D. S., & Shustov, B. M. 2002, ApJ, 569, 792

Lis, D. C., Roueff, E., Gerin, M., Phillips, T. G., Coudert, L. H., van der Tak, F. F. S., & Schilke, P. 2002, ApJ, 571, L55

Loinard, L., Castets, A., Ceccarelli, C., Tielans, A. G. G. M., Faure, A., Caux, E., & Duvert, G. 2000, A&A 359, 1169

Ohashi, N. 2000, in Astrochemistry: From Molecular Clouds to Planetary Systems, IAU Symposium 197, ed. Y. C. Minh, & E. F. van Dishoeck (Astronomical Society of the Pacific), 61

Parise, B., Ceccarelli, C., Tielens, A. G. G. M., Herbst, E., Lefloch, B., Caux, E., Castets, A., Mukhopadhyay, I., Pagani, L., Loinard, L. 2002, A&A, 393, L49

Penston, M. V. 1979, MNRAS, 144, 425

Pratap, P., Dickens, J. E., Snell, R. L., Miralles, M. P., Bergin, E. A., Irvine, W. M., & Schloerb, F. P. 1997, ApJ 486, 862

Roberts, H., & Millar, T. J. 2000, A&A, 364, 780

Roberts, H., Herbst, E., & Millar, T. J. 2003, ApJ, 591, L41

Roueff, E., Tiné, S., Coudert, L. H., Pineau des Forets, G., Falgarone, E., & Gerin, M. 2000, A&A, 354, L63

Shematovich, V. I., Wiebe, D. S., Shustov, B. M., & Li, Z.-Y. 2003, ApJ, 588, 894

Suzuki, H., Yamamoto, S., Ohishi, M., Kaifu, N., Ishikawa, S.-I., Hirahara, Y., & Takano, S. 1992, ApJ, 392, 551

Tafalla, M., Myers, P. C., Caselli, P., Walmsley, C. M., & Comito, C. 2002, ApJ, 569, 815

Tafalla et al. 2003, submitted to ApJ

Terzieva, R. & Herbst, E. 1998, ApJ, 501, 207

van der Tak, F. F. S., Schilke, P., Muller, H. S. P., Lis, D. C., Phillips, T. G., Gerin, M., & Roueff, E. 2002, A&A, 388, L53

Ward-Thompson, D., Scott, P. F., Hills, R. E., & André, P. 1994, MNRAS, 268, 276

Ward-Thompson et al. in this volume

Willacy, K., Langer, W. D., & Velusamy, T. 1998, ApJ, 507, L171